Computational Chemistry: A Way To Reach Spectroscopic and Thermodynamic Data for Exotic Compounds

Frédéric Bouyer,[†] Gérard Picard,*,[†] and Jean-Jacques Legendre

Laboratoire d'Électrochimie et de Chimie Analytique (URA 0216), and Laboratoire de Modélisation Appliquée à la Chimie et aux Procédés, École Nationale Supérieure de Chimie de Paris, 11, rue Pierre et Marie Curie, 75231 PARIS, Cedex 05, France
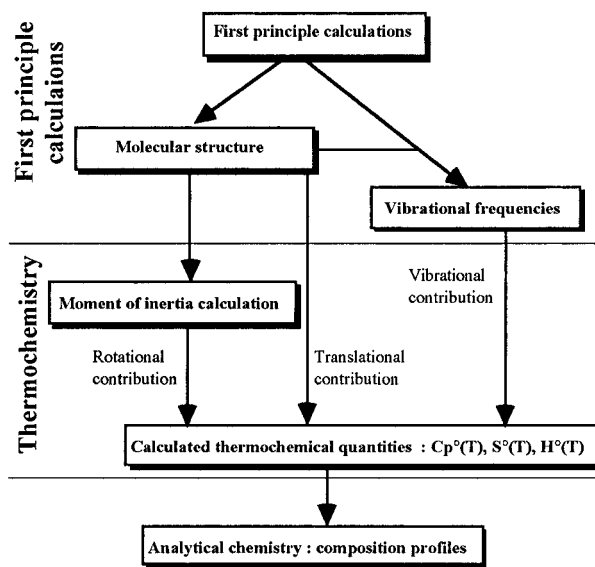
In this paper, we report a general methodology to reach thermochemical properties of molecules in gas phase. We applied these calculations to related complexes of industrial interest, concerning the electrowinning of aluminum. This thermochemical prediction is a demonstration of a quantitative analysis after geometry optimizations and frequencies calculations from density functional computations (or any first-principle techniques). Since this methodology is completely generic, we can study any complexes of interest in order to study the model of the vapor. We have especially investigated the (Na_3AlF_6, Na_2AlF_5, $NaAlF_4$, AlF_3, NaF, $(NaF)_2$, $(NaAlF_4)_2$) system. It has been found that $NaAlF_4$ and $(NaF)_2$ are the major species present in gas phase. Results concerning calcium are also presented, showing that $CaAlF_5$ is in the vapor. Its partial pressure decreases when the one of CaF_2 increases and the partial pressure of $NaAlF_4$ (and all minor species containing aluminum) decreases at the same time.

INTRODUCTION

The prediction of molecular properties from computer simulations is playing an increasing role in the field of inorganic chemistry. Thanks to the theoretical developments in implementation and recent evolution of computers, quantum chemistry calculations become more tractable and routine. Recently, we have developed in our laboratory such theoretical investigations as an analytical tool for chemistry investigations in molten media. In fact, molten salts have two main advantages: the first one is the wide choice for chemical and electrochemical properties and melting points to perform suitable processes, the second advantage is that molten systems exhibit appreciable solubility of metals, making them good solvents for electrometallurgy, electrorefining, and electrowinning processes.

The so-called first-principle computations (Hartree−Fock and Density Functional) allow a structural study of entities of interest for the chemist and the determination of all electronic properties through quantum chemistry. We can see a growing literature concerning theoretical calculations, geometry optimizations, and conformation analyses to the help of the understanding of structures of studied solutions. However the thermochemical analyses are still lacking.

Thermochemical analyses can be useful for the chemist to study reactions and predict compositions. However thermochemistry in liquid phase is unreachable, except by the use of molecular dynamics techniques (quantum dynamics[1,2]) for which hardware requierements are considerable. Nevertheless, we have recently obtained in our laboratory an accurate model to predict the composition of cryolite by calculating reaction constants.[3] In general, using first principle techniques applied to clusters involves the omission of the influence of temperature on the enthalpy and entropy.

* To whom correspondence should be addressed−e-mail: picard@ext.jussieu.fr URL home of the laboratory : http://alcyone.enscp. jussieu.fr/Pages/LECA/GP/.
    † Laboratoire d'Electrochimie et de Chimie Analytique.
    ‡ Laboratoire de Modélisation Appliquée à la Chimie et aux Procédés.
    ⊗ Abstract published in *Advance ACS Abstracts,* April 15, 1996.

Figure 1. Scheme of thermochemical calculations for molecules in gas phase.

Thermochemistry in the gas phase is reachable in almost all cases after studying compounds by quantum mechanical computations. This is the purpose of the present paper. In fact, most of the DFT software we used do not propose thermochemical analysis. Therefore, we have developed a small program[4,5] (using the Mathematica software) which calculates all thermochemical quantities for the molecules of interest. We have checked the consistency of this program on well-known entities, but the goal is to determine properties of unknown compounds and to predict the compositions of related gas phase.
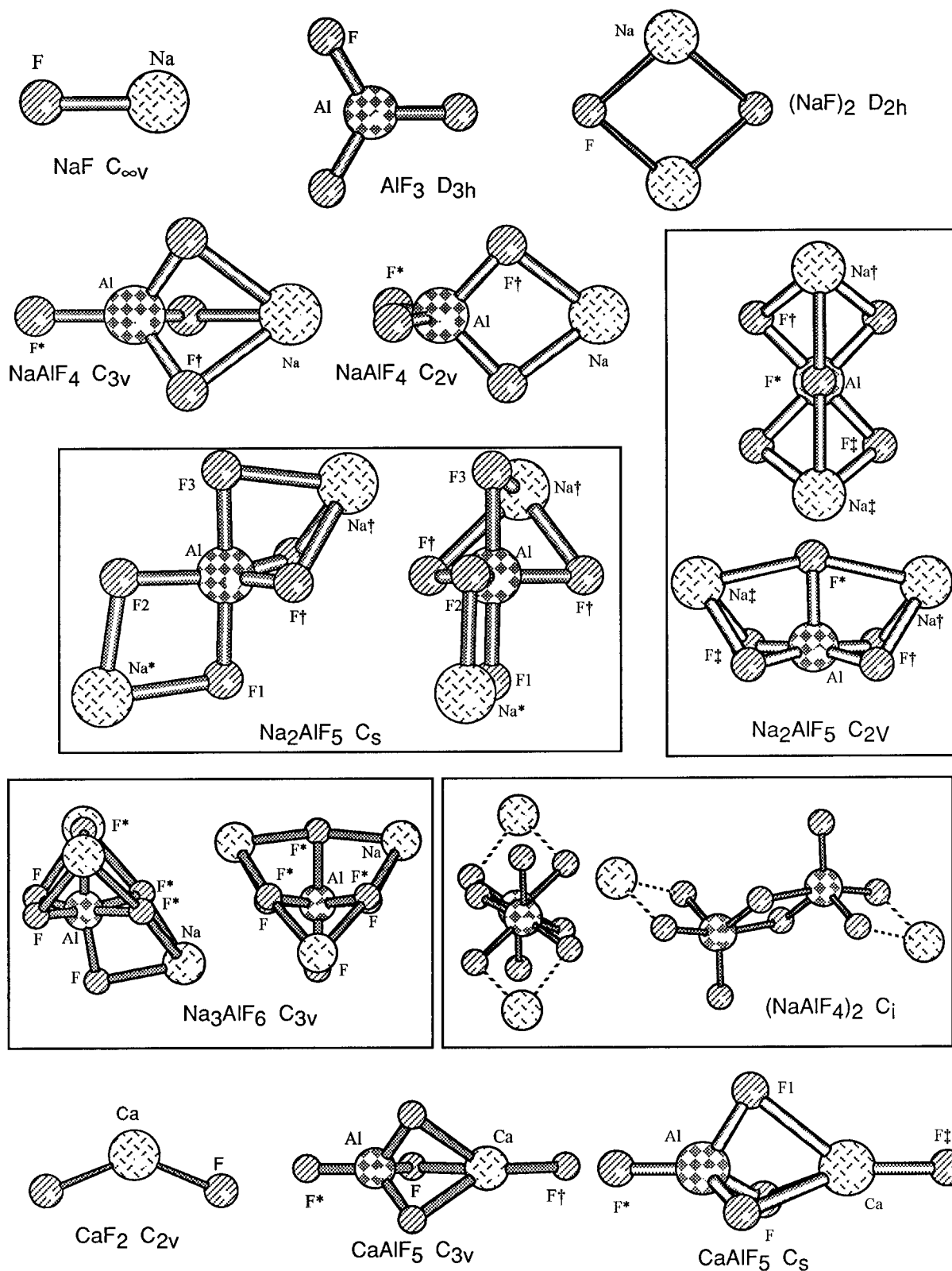
COMPUTATIONAL ELEMENTS

In this part, all relations used in our program are in reference 6 and 7. Calculations of thermochemical quantities

COMPUTATIONAL CHEMISTRY

J. Chem. Inf. Comput. Sci., Vol. 36, No. 4, 1996 **685**

Figure 2. Structures of the most important complexes to be considered in gas phase.

involve the use of quantum statistics, but to obtain numerical solution, we used classical statistics. These calculations imply contributions of either rotational, translational, vibrational, and electronic levels for an ideal monoatomic or diatomic gas and a linear and nonlinear molecule. The algorithm is depicted on the Figure 1, showing the separate approach between quantum mechanical and thermochemical calculations.

For a monatomic gas, translational and electronic contributions are only present. It involves calculations of electronic energy levels and their quantum weights.

In an ideal gas, the structure of the considered molecule is required. Geometry optimization and vibrational frequencies are also necessary. With these structural and vibrational data, we can calculate all contributions of all thermochemical quantities, considered as functions of temperature. The

Table 1. Comparison of Principal Moments of Inertia for AlF_3

principal moments of inertia (10^{-39} g cm^2)	I_a	I_b	I_c
JANAF[6]	12.5730	12.5730	25.1460
LDA-JMW	12.8546	12.8546	25.7094
NLDA-BLYP	13.2102	13.2102	26.4204

Table 2. Comparison of Principal Moments of Inertia for $NaAlF_4$ (C_{2v} and C_{3v} Tridentate Symmetries)

| principal moments of inertia (10^{-39} g cm^2)	I_a	I_b	I_c
JANAF (C_{2v})[6]	24.1060	44.4685	44.5470
LDA-JMW C_{3v}	20.9225	43.4637	43.4637
LDA-JMW C_{2v}	23.1513	46.8208	49.4833
NLDA-BLYP C_{3v}	21.8729	45.4811	45.4811
NLDA-BLYP C_{2v}	23.8690	49.1851	51.7112
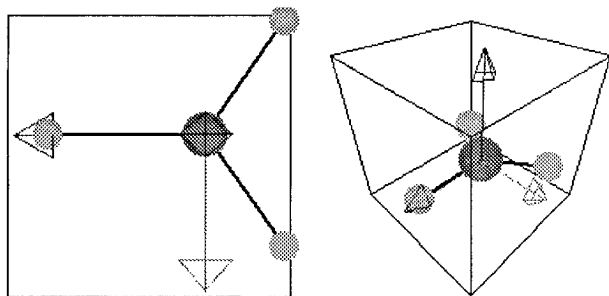
Figure 3. Eigenvectors of inertia matrix for AlF_3 (D_{3h}).
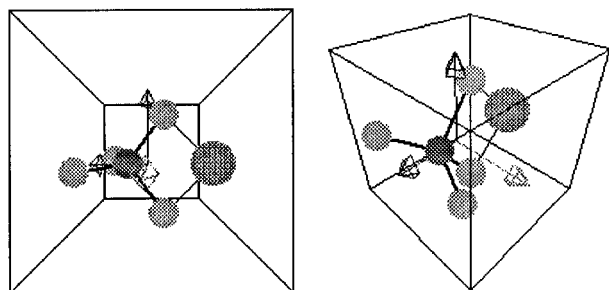
Figure 4. Eigenvectors of inertia matrix for $NaAlF_4$ (C_{2v}).

computational part can be found in ref 6. Rotational contribution needs the calculus of principal moments of inertia, which is depicted in the present paper.

With the help of thermochemical analysis, it is possible to reach free enthalpies of reactions at the temperature of interest and thus to derive the reaction constants. Thanks to these equilibrium constants, all possible reactions (which constitute the model of the vapor) are taken into account from a chemical analysis, based on equilibrium constants and conservation equations applied to molecular vapor species on a neutralizing background. Thermochemical analyses have been first applied to study cryolitic melts and vapor phase (which is the subject of the present paper) over the molten cryolite,[5] the LiCl-MCl (M = Na, K, Rb) molten salts[8] and complex chemistry in vapor phase.[9]

RESULTS

The goal of this work is to analyze the gas phase in equilibrium with molten cryolitic melts which are the media used for the industrial production of aluminum. We will demonstrate how computational chemistry allows one to reach the energetic and structural aspects for the reactivity in ionic liquids.
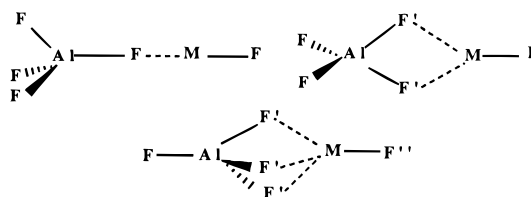
Figure 5. Three possible structures of $CaAlF_5$, emphasized by Curtiss and Heinricher (C_{3v} monodentate, C_{2v}, and C_{3v} tridentate).[21]

Table 3. Total Energy and Free Enthalpy (at 1280 K) Differences between C_{3v} $CaAlF_5$ and C_s $CaAlF_5$ for Several Basis Sets

basis sets	total energy difference (C_s-C_{3v})	free enthalpy difference (C_s-C_{3v}) at 1280 K
STO-3G*	2.2 kJ/mol	
STO-6G*	6.9 kJ/mol	
3-21G*	−1.6 J/mol	−11.375 kJ/mol
TZV	−2.4 J/mol	−11.553 kJ/mol

We first studied all structures that could be present in the gas phase. Our theoretical calculations were performed at the LDA (local density approximation) and NLDA (nonlocal density approximation) levels of computation with the DMol software.[10−12] We have previously tested this software for the study of molten salts,[13−16] which are used in the electrorefining process of aluminum. The hamiltonians taken for both levels of calculations are one of Janak, Morruzi, and Williams (called JMW for short, at the LDA level)[17] and one of Becke and Lee-Yang and Parr (called BLYP for short, at the NLDA level)[18] (at each step of the SCF procedure). The DFT technique was chosen over the Hartree−Fock (HF) one because of its speed performance on large systems, N^3 for DFT methodologies while correlated Hartree−Fock methods giving results of similar quality scale with N^5 (N stands for the size of the basis set).

First of all, we obtained structures of all complexes that could be present in the vapor: NaF ($C_{\infty v}$ symmetry), AlF_3 (D_{3h}), $NaAlF_4$ (C_{2v} and C_{3v}), Na_2AlF_5 (C_{2v} and C_s), Na_3AlF_6 (C_{3v}), $(NaF)_2$ (D_{2h}), $(NaAlF_4)_2$ (C_i), CaF_2 (C_{2v}) and $CaAlF_5$ (C_{3v} and C_s). Then, vibrational frequencies have been computed that can give a comparison element between quantum chemistry calculations and IR or Raman spectroscopic data. Finally the statistical thermochemistry software[4] was applied to all studied complexes.

Structural Analyses. We have modeled the most important complexes[19] of cryolitic vapor phase, and we have obtained both structures and vibrational frequencies. Structures are depicted in Figure 2. The presented geometries do not contain all bond lengths as well as angles, which will be the subject of a forthcoming paper. For some entities, several conformations have been determined. In fact, $NaAlF_4$ has been studied[20] by Scholz and Curtiss who obtained three different conformations: the C_{3v} symmetry, in which sodium is in a monodentate position, the C_{2v} symmetry (Na in a bidentate position), and C_{3v} symmetry (Na in a tridentate position). The C_{2v} monodentate geometry of $NaAlF_4$ is the less stable structure, if we retained the 6-31+G*, at the MP2//HF level of computation. Considering their results, we retained only the C_{2v} and C_{3v} (tridentate) symmetries for our theoretical investigations. All calculations were done at the LDA and NLDA level of computation with the DNP basis sets (double numeric plus polarization functions, quite similar to the DZP or 6-31G** Gaussian basis sets), which do not include diffuse functions, and more complex models (com-

COMPUTATIONAL CHEMISTRY

J. Chem. Inf. Comput. Sci., Vol. 36, No. 4, 1996 **687**

Table 4. Total Energies in au of Related Complexes

complexes/total energies	LDA-JMW	NLDA-BLYP
NaF ($C_{\infty v}$)	−260.76234	−262.23326
AlF$_3$ (D_{3h})	−539.41497	−542.33291
NaAlF$_4$ (C_{2v})	−800.31565	−804.68486
NaAlF$_4$ (C_{3v})	−800.31633	−804.68344
Na$_2$AlF$_5$ (C_{2v})	−1061.16677	−1066.98054
Na$_2$AlF$_5$ (C_s)	−1061.16620	−1066.98184
Na$_3$AlF$_6$ (C_{3v})	−1322.03661	−1329.29997

Table 5. Constants of the Reactions in Gas Phase at the Temperature of 1280 K

reactions	LDA-JMW	NLDA-BLYP
NaF + AlF$_3$ → NaAlF$_4$	$K_1 = 5.537 \times 10^7$	$K_1 = 4.87 \times 10^5$
2NaF + AlF$_3$ → Na$_2$AlF$_5$	$K_2 = 5.291 \times 10^9$	$K_2 = 8.992 \times 10^4$
3NaF + AlF$_3$ → Na$_3$AlF$_6$	$K_3 = 2.356 \times 10^{11}$	$K_3 = 4.824 \times 10^3$
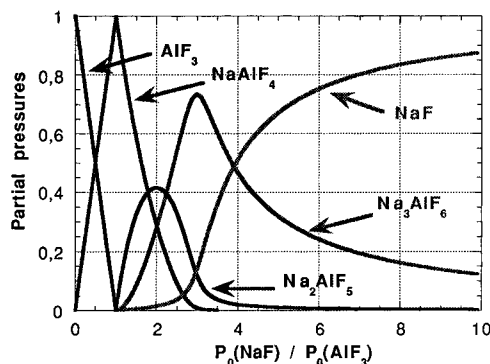
Figure 6. Composition analysis of the vapor for the (Na$_3$AlF$_6$, Na$_2$AlF$_5$, NaAlF$_4$, AlF$_3$, NaF) system at 1280 K from the LDA results.
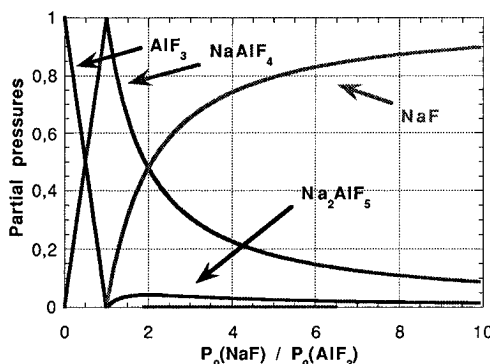
Figure 7. Composition analysis of the vapor for the (Na$_3$AlF$_6$, Na$_2$AlF$_5$, NaAlF$_4$, AlF$_3$, NaF) system at 1280 K from the NLDA results.

pared to the anionic one[15]) have to be proposed[3] to treat complexes in liquid cryolite.

Several conformations have been initally used for geometry optimizations for exploring potential energy surfaces for all systems. The optimized structures were obtained at the two levels of calculations (local and nonlocal approximations), showing that all bond lengths from NLDA structures are slightly wider than the ones from LDA results. It is well-known that the LDA calculations overestimate binding energies that affect naturally all bond lengths. More accurate reaction energies are obtained at the NLDA level, which we will see below. Another interesting feature is the structure of CaAlF$_5$, in which the calcium cation is not located around the complex but is part of the whole structure. This geometry can be viewed as a "bimetallic" complex, in which calcium could be the second "metallic atom".
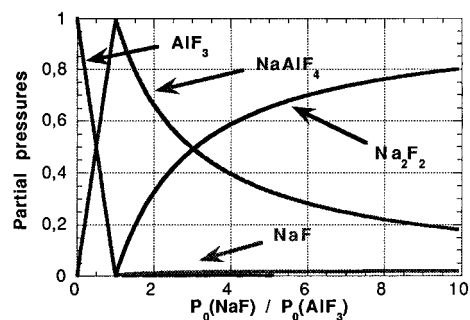
Figure 8. Composition analysis of the vapor for the (Na$_2$AlF$_5$, NaAlF$_4$, AlF$_3$, NaF, (NaF)$_2$, (NaAlF$_4$)$_2$) system at 1280 K from the NLDA results.

Statistical Thermochemistry. All structural and vibrational data are taken from the previous density functional calculations, and we compute translational, vibrational, and rotational contributions of thermochemical quantities. Furthermore, for the rotational part, principal moments of inertia have been calculated, and the eigenvectors of the inertia matrix are represented. The principal moments I_a, I_b, and I_c can be a purely structural comparison standpoint, if they are known. For AlF$_3$ and NaAlF$_4$, we present the calculated moments of inertia, reported in Tables 1 and 2. Moments of inertia are depicted in Figures 3 and 4 for AlF$_3$ (D_{3h}) and NaAlF$_4$ (C_{2v}) complexes. An example of outputs of an thermochemical calculation is reported in the annexe (concerning CaAlF$_5$, C_s symmetry).

From the analysis of S°(T), H°(T), and G°(T), we have established that these quantities change between 0.01 and 7%, depending on the temperature (in the range of 100−1300 K), the size of the molecule (from NaF to Na$_3$AlF$_6$ for example), and the change on the structures of molecules (increasing all bond lengths between 0.01 to 0.03 Å) and their frequencies (if we add or subtract 50 cm^{-1} to all frequencies). Concerning vibrational analyses, it has to be pointed out that changes in vibrational frequencies strongly affect all calculated quantities and produce the most significant modifications in thermochemical functions (especially if there are frequencies of low energy): it means that all structures must be optimized with drastic threshold values on gradients in order to obtain reliable vibrational frequencies.

In any way, if we are aware of these problems, it is possible to derive correct thermochemical functions from structural data and vibrational frequencies.

Concerning NaAlF$_4$, we can sum up our theoretical investigations by stating that HF/6-31G* calculations can be compared to ones of the DNP/LDA level and MP2/6-31+G* results are similar to ones of the DNP/NLDA level of computations by Scholz and Curtiss,[20] who obtained at the HF/6-31G* level a more stable C_{3v} structure (Na tridentate) than the C_{2v} one. According to them, the MP$_2$ level of calculations gives the opposite conclusion. What these authors forgot is the effect of the temperature on the free enthalpy: at high temperature, the C_{2v} structure is more stable than the C_{3v} conformer. The MP$_2$ calculations allow only the conclusion that even at low temperature the C_{2v} structure is more stable than the C_{3v} geometry. We obtained these conclusions with our DFT computations: the LDA level reproduces the HF/6-31G* calculations, and the NLDA level gives similar results to ones of the MP2/6-31+G* computations.

Chart 1

Example of outputs for CaAlF₅ (Cₛ) (NLDA-BLYP) (truncated) :

```
*** Calculs des grandeurs thermochimiques ***

Données de simulation provenant de DMol

Rappels des valeurs utilisées :

Masse molaire: 162.01 g/mol
Masses molaires (g/mol) et coordonnées des atomes (Å) :
    18.9900    0.1019   -0.8118   -1.2971
    26.9800    1.1924   -0.3476    0.0000
    18.9900   -3.3993    0.9980    0.0000
    18.9900    2.7995   -0.8116    0.0000
    18.9900    0.7244    1.3462    0.0000
    18.9900    0.1019   -0.8118    1.2971
    40.0800   -1.5208    0.4387    0.0000
Nombre de symétrie : 1
La molécule n'est pas linéaire
Moments d'inertie :    0.0277193    0.0277207    0.131939 en cm-1
Moments d'inertie :  100.986470     100.981586       21.216398
10-39 en g cm2
Fréquences de vibrations : (en cm-1)
 45.4  50.4  131.7 132.5 221.5
 222.8 232.5 297.9 298.2 352.5
 581.8 617.3 660.1 660.6 889.6

Energie de vibrations à 0 K : 32.2681 kJ/mol
H°(298.15 K) :   26.808 kJ/mol
```

Temp. (K)	Cap. cal. J/K/mol	Entropie J/K/mol	Enthalpie(H°-H°298) kJ/mol	G(T) kJ/mol	Temp. (K)	Cap. cal. J/K/mol	Entropie J/K/mol	Enthalpie(H°-H°298) kJ/mol	G(T) kJ/mol
100					600				
Vibr.	45.494	37.276	2.169		Vibr.	114.574	187.570	49.163	
Rot.	12.472	108.360	1.247		Rot.	12.472	130.706	7.483	
Trans.	20.786	149.489	2.079		Trans.	20.786	186.733	12.472	
Total:	78.751	295.125	5.495(-21.313)	-24.018	Total:	147.831	505.008	69.118(42.310)	-233.887
120					700				
Vibr.	53.345	46.281	3.159		Vibr.	117.030	205.428	60.752	
Rot.	12.472	110.633	1.497		Rot.	12.472	132.628	8.730	
Trans.	20.786	153.279	2.494		Trans.	20.786	189.937	14.550	
Total:	86.602	310.193	7.150(-19.658)	-30.073	Total:	150.288	527.994	84.032(57.224)	-285.564
140					800				
Vibr.	60.215	55.031	4.296		Vibr.	118.709	221.172	72.544	
Rot.	12.472	112.556	1.746		Rot.	12.472	134.294	9.977	
Trans.	20.786	156.483	2.910		Trans.	20.786	192.713	16.629	
Total:	93.473	324.070	8.952(-17.856)	-36.418	Total:	151.966	548.178	99.150(72.342)	-339.393
160					900				
Vibr.	66.303	63.477	5.563		Vibr.	119.900	235.226	84.478	
Rot.	12.472	114.221	1.995		Rot.	12.472	135.763	11.224	
Trans.	20.786	159.259	3.326		Trans.	20.786	195.161	18.707	
Total:	99.560	336.957	10.884(-15.924)	-43.029	Total:	153.158	566.150	114.409(87.601)	-395.125
180					1000				
Vibr.	71.747	71.606	6.944		Vibr.	120.774	247.906	96.514	
Rot.	12.472	115.690	2.245		Rot.	12.472	137.077	12.472	
Trans.	20.786	161.707	3.741		Trans.	20.786	197.351	20.786	
Total:	105.005	349.004	12.930(-13.878)	-49.890	Total:	154.032	582.334	129.771(102.963)	-452.563
200					1100				
Vibr.	76.637	79.423	8.429		Vibr.	121.433	259.450	108.626	
Rot.	12.472	117.004	2.494		Rot.	12.472	138.265	13.719	
Trans.	20.786	163.897	4.157		Trans.	20.786	199.332	22.865	
Total:	109.895	360.325	15.080(-11.728)	-56.985	Total:	154.691	597.047	145.209(118.401)	-511.543
300					1200				
Vibr.	94.490	114.202	17.067		Vibr.	121.941	270.038	120.795	
Rot.	12.472	122.061	3.741		Rot.	12.472	139.350	14.966	
Trans.	20.786	172.325	6.236		Trans.	20.786	201.141	24.943	
Total:	127.748	408.589	27.044(0.236)	-95.532	Total:	155.199	610.530	160.705(133.897)	-571.931
400					1300				
Vibr.	104.755	142.925	27.076		Vibr.	122.340	279.815	133.010	
Rot.	12.472	125.649	4.989		Rot.	12.472	140.349	16.213	
Trans.	20.786	178.305	8.314		Trans.	20.786	202.805	27.022	
Total:	138.013	446.879	40.379(13.571)	-138.373	Total:	155.598	622.969	176.245(149.437)	-633.614
500					1400				
Vibr.	110.813	167.008	37.880		Vibr.	122.660	288.894	145.261	
Rot.	12.472	128.432	6.236		Rot.	12.472	141.273	17.460	
Trans.	20.786	182.943	10.393		Trans.	20.786	204.345	29.100	
Total:	144.071	478.383	54.508(27.700)	-184.683	Total:	155.918	634.512	191.822(165.014)	-696.495

Concerning Na₂AlF₅, the C_{2v} structure is more stable at low temperature than the C_s geometry, at the LDA level. At high temperature, the C_s symmetry is more stable. At the NLDA level, this structure is always more stable than the other at all temperatures.

The case of CaAlF₅ complexe is quite similar. Curtiss and Heinricher[21] have shown that the C_{3v} monodentate structure is more stable than the others (depicted in Figure 5).

These conclusions were taken from HF/STO-3G level of calculations. We have verified this assumption using DMol with stronger threshold values on gradients, showing at the NLDA level the stability of the C_s symmetry structure compared to the C_{3v} one. Moreover, we completely verified this assumption using the GAMESS software[22] from Dr. Mark Gordon's Research Group. We completely optimized (with either MacGamess or Gamess on SGI) CaAlF₅ under symmetry constrain (both C_{3v} and C_s) with several basis sets.

Total energies, energy and free enthalpy differences (at 1280 K) are reported in Table 3 for the two conformers (C_s and C_{3v} symmetry structures).

The HF/STO-3G* and HF/STO-6G* levels of calculations emphazise two imaginary frequencies, leading to an unstable conformation for the C_{3v} symmetry structure, even if strong threshold values on gradients (10^{-5} Ha/Bohr) are used. Nevertheless, the total energies could be employed for evaluating reaction energies at 0 K, because decreasing all convergence criteria do not produce significant energy changes (about or less 10^{-6} Ha).

Trends emerge from the analysis of total energies and free enthalpies calculated at 1280 K with Gamess. The C_s symmetry geometry is always more stable, except for the two first basis sets (considered as minimal basis sets) for which there is a few kJ/mol of energy difference, that could not be significant from a chemical point of view. Since imaginary frequencies arise from the two first basis sets, it is not possible to accurately calculate free enthalpies for the C_{3v} symmetry structure. Nevertheless, for the two last basis sets (containing more atomic orbitals since all valence functions are doubly or triply splitted), the free enthalpy differences show that the C_s conformer is more stable that the C_{3v} symmetry structure at 1280 K (as for all temperatures in the range of 500−1400 K). Based on Hartree−Fock calculations, it is then established that the CaAlF$_5$ C_s conformer is the one which is present in the gas phase.

Our theoretical investigations show that at the NLDA level the C_{3v} structure is not stable (one imaginary frequency). As we have noticed before, if we use stronger threshold values on gradients, we obtain a C_s structure of CaAlF$_5$: this symmetry is very important, since the symmetry number directly appears in thermochemical functions and strongly affects these data. The energy of CaAlF$_5$ C_s is slightly lower, and the free enthalpy difference between these two conformations is 12 kJ/mol in favor of the C_s symmetry (comparable to the free enthalpy differences derived from Hartree−Fock calculations with Gamess). The consequence on the reaction constant of the following reaction

$$AlF_3 + CaF_2 \leftrightarrow CaAlF_5$$
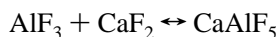
is that it changes from 639 to 1910 at 1280 K. From our investigations, we retain the C_s structure of CaAlF$_5$.

Equilibrium Reactions in Gas Phase. It is clear that with the entropy and enthalpy of the complex, the enthalpy, and free enthalpy of reaction can be calculated. We have taken into account the zero point energy into our calculations. The relation used is the following

$$\Delta H_r^0(T) = \sum_{products} (H_{DFT}(0K) + ZPE) - \sum_{reactive\ species}$$
$$(H_{DFT}(0K) + ZPE) + \sum_{products} H^0(T) - \sum_{reactive\ species} H^0(T)$$

where $H_{DFT}(0K)$ is the total energy computed by any quantum chemical software (at present, by DFT-DMol), $H^0(T)$ contains all contributions described in annex, and

$$ZPE = H_{vib}(0K) = \frac{1}{2} \sum_{normal\ modes} h\nu_i$$

for the proper compound.

In the same way

$$\Delta G_r^0(T) = \Delta H_r^0(T) - T(\sum_{products} S^0(T) - \sum_{reactive\ species} S^0(T))$$

and the constant of reaction is then calculated from the relation

$$\Delta G_r^0(T) = RT \ln K_r$$

By classical statistics, enthalpies and entropies are calculated according to ref 6. The relations for the enthalpy and entropy used in ref 4 are (assuming that at 0 K these quantities are equal to zero)

$$S^0(T) - S^0(0K) = R\left(\frac{5}{2} + \frac{5}{2}\ln T + \frac{3}{2}\ln M + \right.$$
$$\ln \frac{k}{p^0}\left(\frac{2\pi k}{Nh^2}\right)^{3/2}\right) + R\sum_{i=1}^{3n-6}\left(\frac{\nu_i e^{-\nu_i}}{1 - e^{-\nu_i}} - \ln(1 - e^{-\nu_i})\right) + \frac{3}{2}R +$$
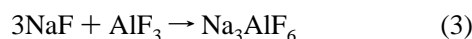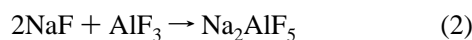$$\frac{R}{2}\ln\left(\frac{\pi\sigma}{I_a I_b I_c}\right)$$

$$H^0(T) - H^0(0K) = \frac{5}{2}RT + RT\sum_{i=1}^{3n-6}\frac{\nu_i e^{-\nu_i}}{1 - e^{-\nu_i}} + \frac{3}{2}RT$$

These relations are those of polyatomic nonlinear molecules, in which the first term refers to the translational contribution, the summation over all frequencies ν_i ($1 \le i \le 3n-6$), for a molecule constituted of n atoms, represents the vibrational contribution, and the last term corresponds to the rotational contribution. M refers to the molecular weight, I_a, I_b, and I_c principal moments of inertia, N the Avogadro number, σ the symmetry number, and p^0 the standard pressure. All these relations (the ones of diatomic, polyatomic linear, and nonlinear molecules) are computed for each complex and then are used to calculate reactions constants.

All computed values we used to calculate reaction constants are reported in Table 4.

All structural details will be the subject of a forthcoming paper and will be discussed elsewhere. For computing reaction enthalpies, we tested several conformers in some cases in order to decide which one will be the most stable at the temperature of interest.

On the basis of our results, we have obtained constants of the following reactions at the temperature of 1280 K (around the temperature of the industrial aluminum electrowinning process).

$$NaF + AlF_3 \rightarrow NaAlF_4 \qquad (1)$$

$$2NaF + AlF_3 \rightarrow Na_2AlF_5 \qquad (2)$$

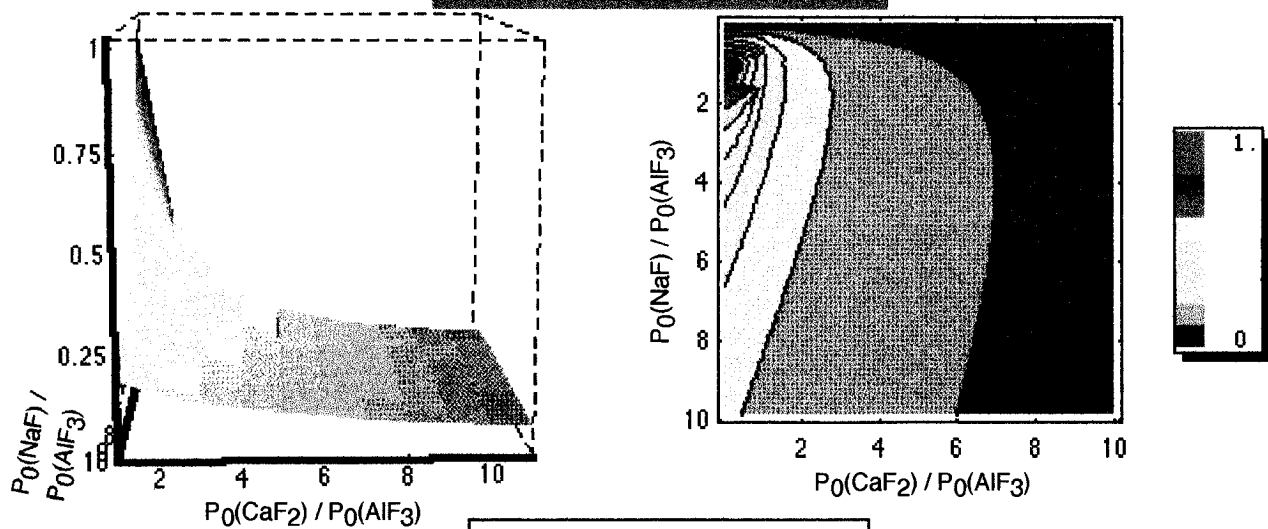$$3NaF + AlF_3 \rightarrow Na_3AlF_6 \qquad (3)$$

Trends and remarks emerge from these results. These thermochemical analyses point out that reaction constants are very high and differed from either one level of computa-

Partial pressure of Na₂AlF₅
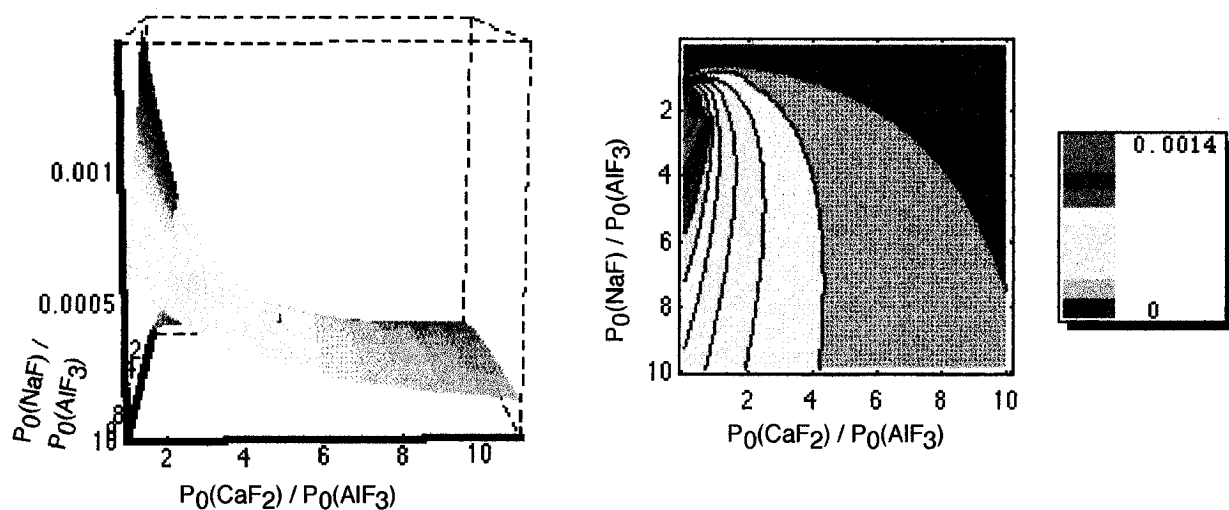
Partial pressure of NaAlF₄
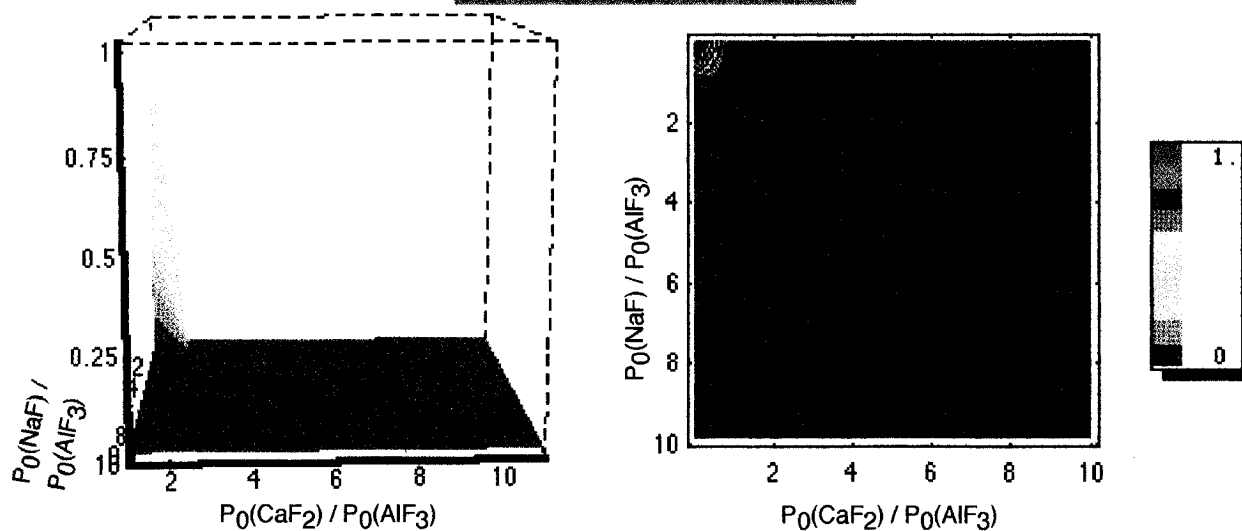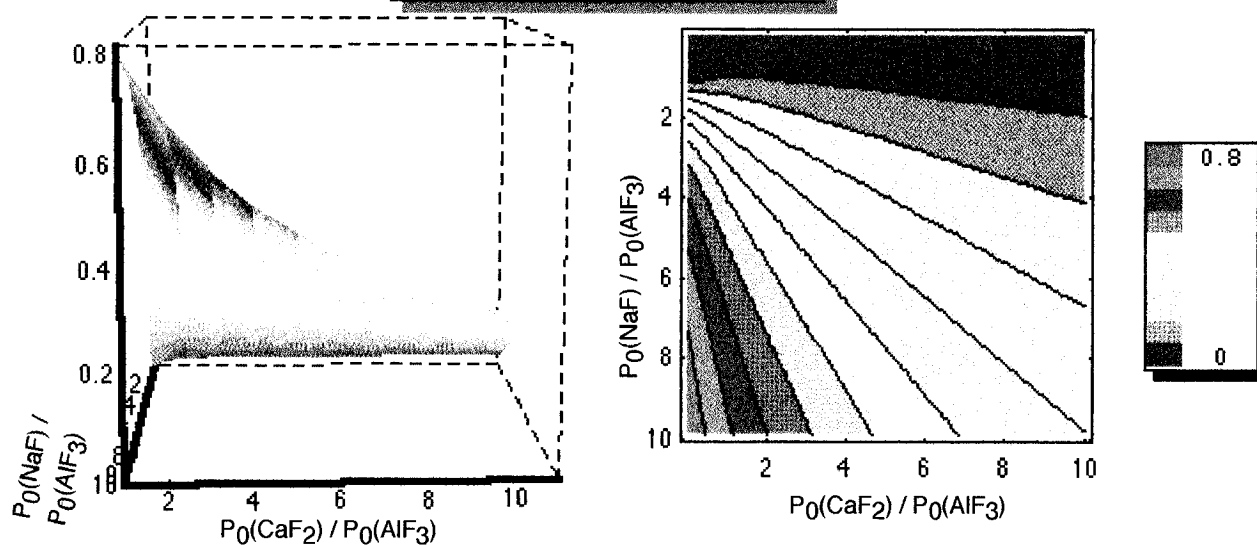

Partial pressure of AlF₃
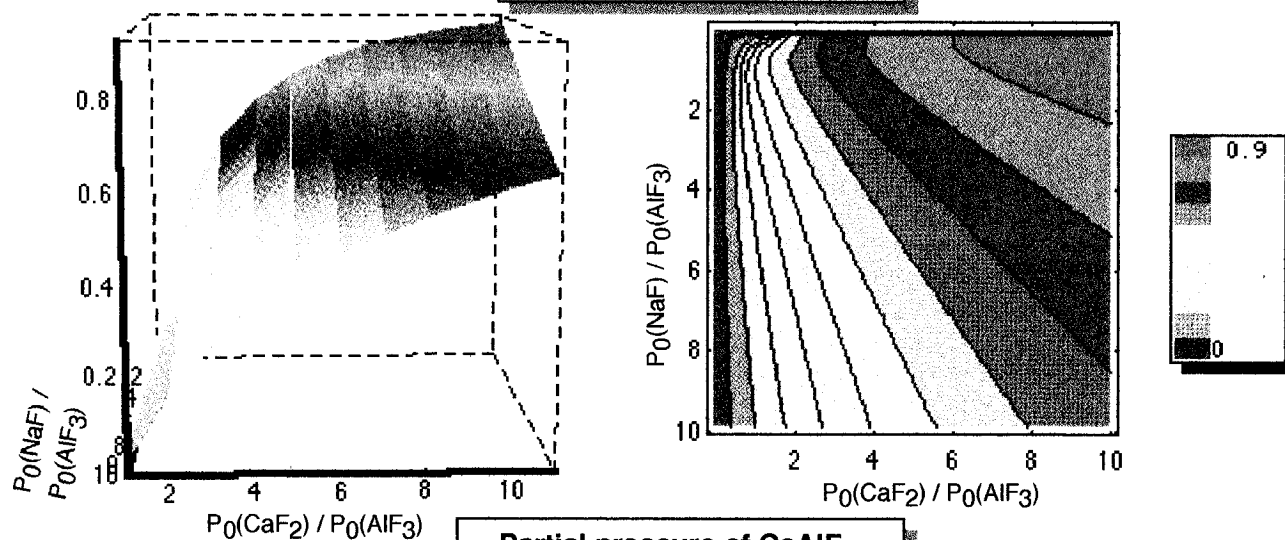

Figure 9. Partial pressures of complexes.

tion to another. The consequence is that the final predicted vapor composition is strongly affected. In fact, at the local level of computation Na_3AlF_6 should be formed when it should not if we retain non-local results.

COMPUTATIONAL CHEMISTRY
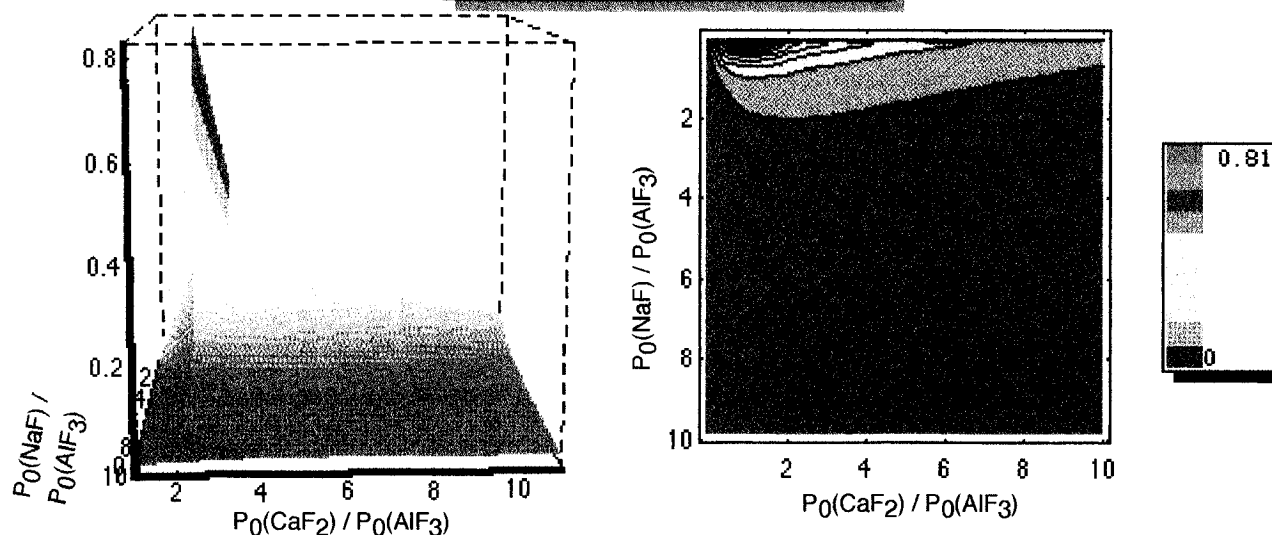
J. Chem. Inf. Comput. Sci., Vol. 36, No. 4, 1996 **691**

Figure 10. Partial pressures of complexes.

To visualize these values, we have represented the vapor composition versus the pressure ratio, $P_0(NaF)/P_0(AlF_3)$. We have resolved the equation system constituted by equations of conservation and equilibrium constants. Finally, we have

692 *J. Chem. Inf. Comput. Sci., Vol. 36, No. 4, 1996*

PICARD ET AL.

plotted the results, depicted by Figures 6 and 7 for each level of calculations.

In the literature, Vajna and Bacchiega[19,23] have pointed out results concerning vapor compositions above cryolitic melts, in terms of the cryolitic ratio defined by the concentration ratio of (NaF) over (AlF$_3$) in the molten mixture. At the NaAlF$_4$ composition (cryolitic ratio of 1), the vapor contains NaAlF$_4$ only. For melts with a cryolitic ratio higher than 1, the vapor contains NaAlF$_4$ and NaF. Finally, for melts of cryolitic ratio less than 1, the vapor contains NaAlF$_4$ and AlF$_3$. Our results, based on a theoretical approach, are in agreement with the experimental observations, if we consider NLDA-BLYP values. These two curves, presented here, show clearly the tendencies of the local and nonlocal levels of calculations. Local computations tend to overestimate reaction energies, while nonlocal calculations tend to the more precise results generally. Here, the Na−F bond strength is overestimated, since the bond length is smaller at the local level. Generally LDA structures can be obtained at a sufficient level of accuracy, but for the energy reactions nonlocal computations are necessary for coming to reliable results to be compared with experimental ones. With the help of the computational chemistry, we have reached accurate equilibrium constants and a reliable composition of the vapor. However, we do not calculate these compositions as a function of the liquid cryolitic ratio but only as a function of calculated partial pressures. Nevertheless, these curves fit the tendencies observed experimentally.

Influence of Some Dimerizations. Since this methodology is completely generic, we have included (NaF)$_2$ and (NaAlF$_4$)$_2$ species in our model. Constants of the following reactions

$$2NaAlF_4 \leftrightarrow (NaAlF_4)_2$$

$$2NaF \leftrightarrow (NaF)_2$$
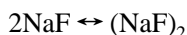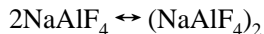
were calculated at 1280 K and are 6.565×10^{-8} and 2318, respectively (from NLDA results). One can imagine easily that the NaAlF$_4$ dimer would be not signicantly present in the vapor, but the presence of (NaF)$_2$ could change the composition analysis, as depicted in Figure 8.

It is clearly shown that the dimer (NaAlF$_4$)$_2$ is not present in the gas phase, but it is surprising to note that it is not NaF but (NaF)$_2$ which is present in the vapor. Since it consumes twice more sodium fluoride, the pentacoordinated aluminum complex Na$_2$AlF$_5$ is less present in the vapor. We do not take into account in this model the possible presence of Na$_3$AlF$_6$, which has already been rejected with the previous model.

On the basis of our theoretical results, NaAlF$_4$ and (NaF)$_2$ are the most significant compounds present in the vapor. The amount of Na$_2$AlF$_5$ does not appear to be as important as in the previous (Na$_3$AlF$_6$, Na$_2$AlF$_5$, NaAlF$_4$, AlF$_3$, NaF) model. With our theoretical methodology, we emphasize the presence of the (NaF)$_2$ dimer.

Effect of the Calcium. The effect of the calcium has been studied theoretically, by applying the whole methodology (DFT and thermochemical calculations) to CaF$_2$ and CaAlF$_5$ and taking finally the reaction constant of 1910 for the reaction AlF$_3$ + CaF$_2$ $\leftrightarrow$ CaAlF$_5$. All constituents were analyzed as functions of $P_0(NaF)/P_0(AlF_3)$ and $P_0(CaF_2)/P_0(AlF_3)$. Therefore we have obtained partial pressure surfaces

for all compounds in three dimensions. These illustrations are presented in Figures 9 and 10.

All complexes containing aluminum have their partial pressure decreased when the pressure of CaF$_2$ increases. The major species that are present in the vapor are (NaF)$_2$ and CaF$_2$, at high partial pressures of NaF and CaF$_2$, if one can reach them. It means that all compounds containing aluminum are not in the gas phase but are present in the condensed phase. We have demonstrated[3] that calcium stabilizes the tetragonal and especially the fivefold coordinated aluminum complex. So calcium reduces all partial pressures of complexes containing aluminum and stabilizes aluminum complexes in either liquid or solid phase.

CONCLUDING REMARKS

We have calculated some molecular properties and especially thermochemical quantities from first principle calculations. Our aim is to show how the calculations are applied to industrial problems and to stress the point that these values are of great importance for predicting reactions in the gas phase. It is clear that this methodology is the consequence of particular models (ideal gas, without molecular interactions) and the use of chemistry quantum techniques. This methodology could be applied to any chemical problem of interest. At the present time, with quantum chemistry and thermochemical computations, we gain more insight into the use of these techniques in the field of chemistry in these particular media. On the basis of our theoretical investigations, we agree with experimental observations, with the advantage of quantitative chemical analysis, which is very difficult to achieve especially in molten salts. Prediction can thus be made for studying particular reactions. We have shown that (NaF)$_2$ and NaAlF$_4$ compose the major part of the vapor over cryolite and that calcium reduces all partial pressures of all compounds containing aluminum.

REFERENCES AND NOTES

(1) Car, R.; Parinello, M. *Phys. Rev. Lett.* **1985**, *55*, 2471.

(2) Salahub, D. R.; Fournier, R.; Mlynarski, P.; Papai, I.; St-Amant, A.; Ushio, J. In *Density Functional Methods in Chemistry*; Labanowski, J. K., Andzelm, J. W., Eds.; Springer-Verlag: New York, 1991; p 77.

(3) Bouyer, F.; Picard, G.; Legendre, J. J. *Int. J. Quant. Chem.* To be published.

(4) The MASTER program for **M**olecular **A**b-initio and **S**tatistical **T**hermodynamics **E**valuation of thermodynamic **R**eactivity, written by Frédéric Bouyer with Mathematica, available by email (bouyer@ext.jussieu.fr or picard@ext.jussieu.fr) or through the Web (http://alcyone.enscp.jussieu.fr/Pages/LECA/GP/FB/software.html).

(5) Bouyer, F. Thesis, Université Pierre et Marie Curie, Paris VI, Paris, 95., Oct 95.

(6) (JANAF Table) Chase, M W.; Davies, C. A.; Downey, J. R.; Frurip, D. J.; McDonald, R. A.; Syverud, A. N. *J. Phys. Chem. Ref. Data*, **1985**, *14*, Supplement 1.

(7) Pacault, A.; In *Éléments de thermodynamique statistique*; Masson et Cie, Ed.; Paris, 1963.

(8) Hébant, P.; Picard, G. S. *J. Mol. Struct.* (THEOCHEM) In press.

(9) Hemery, A.; Picard, G. S.; Sibony, M.; Champin, B. *Int. J. Quant. Chem.* To be published.

(10) Delley, B. *J. Chem. Phys.* **1990**, *92*(1), 508.

(11) Delley, B. *New. J. Chem.*, **1992**, *16*, 1103.

(12) DMol, User Guide; Biosym Technologies: version 2.3.6, 1993.

(13) Bouyer, F.; Picard, G.; Legendre, J. J. *C. R. Acad. Sci. Paris*, Ser. II, **1994**, 455.

(14) Bouyer, F.; Picard, G.; Legendre, J. J. *J. Mol. Struct. (THEOCHEM)* **1995**, *330*, 217.

(15) Bouyer, F.; Picard, G.; Legendre, J. J. *Int. J. Quant. Chem.* **1994**, *52*, 927.

(16) G. S., Picard, F. C., Bouyer, *J. Am. Institute Phys.* **1995**, *4*, 297.

(17) Moruzzi, V. L.; Janak, J. F.; Williams, A. R. in *Calculated Electronic Properties of Metals*; Pergamon: New York, 1978.

(18) Vosko, S. J.; Wilk, L.; Nusair, M. *Can. J. Phys.* **1980**, *58*, 1200.

(19) Grjotheim, K.; Krohn, C.; Malinovsky, M.; Matiasovvsky, K.; Thonstad, J. *Aluminium Electrolysis, Fundamentals of the Hall-Héroult Process*; Aluminium-Verlag: Düsseldorf, 1982.

(20) Scholz, G.; Curtiss, L. A. *J. Mol. Struct. (THEOCHEM)* **1992**, *258*, 251.

(21) Curtiss, L. A.; Heinricher, A. *Chem. Phys. Lett.*, **1982**, *86*(5,6), 467.

(22) Schmidt, M. W.; Baldridge, K. K.; Boatz, J. A.; Elbert, S. T.; Gordon, M. S.; Jensen, J. H.; Koseki, S.; Matsunaga, N.; Nguyen, K. A.; Su, S. J.; Windus, T. L.; Dupuis, M.; Montgomery, J. A. *J. Comput. Chem.*, **1993**, *14*, 1347.

(23) Vajna, A.; Bacchiega, R. *Metal. Ital.* **1960**, *52*, 481.